ON THE THERMALLY-INDUCED RESIDUAL STRESSES IN THICK FIBER-THERMOPLASTIC MATRIX (PEEK) CROSS-PLY LAMINATED PLATES

Shoufeng Hu and John A. Nairn*
Materials Science and Engineering, University of Utah, Salt Lake City, Utah

SUMMARY

An analytical method for calculating thermally-induced residual stresses in laminated plates is applied to cross-ply PEEK laminates. We considered three cooling procedures — slow cooling (uniform temperature distribution), convective and radiative cooling, and rapid cooling by quenching (constant surface temperature). Some of the calculated stresses are of sufficient magnitude to effect failure properties such as matrix microcracking.

INTRODUCTION

Thermally-induced residual stresses in laminated composites are introduced by fabrication and by environmental exposure. They are an unavoidable consequence of (1) the nonuniform distribution of cooling temperature due to the phenomenon of heat transfer and (2) the difference in thermal expansion coefficients of lamina in the fiber direction and the transverse direction. For thin laminated plates the residual stresses caused by (1) may be ignored. But, for thick laminated plates the residual stresses caused by (1) can be as large as those caused by (2). Tensile residual stresses in off-axis plies (*e.g.* 90° plies) are particularly important because they may be large enough to promote damage by matrix microcracking. The prediction and measurement of residual stresses are therefore important topics that are relevant to production, design, and performance of composite components.

Residual (or thermal) stresses and heat transfer are classical problems for conventional materials. A number of investigations specific to composite materials are available (*e.g.* Refs. [1-6]). The theoretical and experimental investigations for residual stresses in Refs. [1-4] and [6] illustrate the residual stresses due to unequal thermal expansion coefficients in the fiber and the transverse directions. Using the finite difference method (for temperature) and finite element method (for thermal stresses), Chen *et. al.* [5] studied the failure of laminates under thermal and mechanical loading with the consideration of heat transfer. But only few investigators have considered the residual stresses caused by the nonuniform distribution of temperature, which is especially significant for thick laminates. The goal of present study is to gain insight into the mechanisms of thermally-induced residual stresses in cross-ply laminates, which are caused by both disparate thermal expansion coefficients and by nonuniform distribution of temperature during cooling.

Thermoplastic matrix (PEEK) composites have received much attention due to their high stiffness and high fracture toughness. The stress-free temperature in PEEK composites was measured to be about 310°C [1,6]. The processing temperature, melting temperature, and crystallization temperature are all above 310°C. We therefore treat PEEK as being fully crystallized at the stress-free temperature and calculate the residual stresses that develop on cooling from the stress-free temperature to room temperature. The problem can be separated into two discrete parts. The first part is the analysis of temperature distribution and the second part is the development of residual stresses for given temperature distribution. The problem is separable because heat transfer is not affected by the presence of residual stresses. We use a coordinate system centered inside the cross-ply laminates having the x-axis aligned with the fiber direction of top ply group and the z -axis perpendicular to plane of the plate.

* Supported in part by a NASA contract NAS1-18833

Our goal is to study the effect of heat transfer on the distribution of the thermally-induced residual stresses. To achieve this goal we consider three cooling procedures: 1) slow cooling in which temperature is uniform over entire thickness and residual stresses are uniform over each laminate group (*i.e.* heat transfer is ignored); 2) cooling under room temperature air by convection and radiation; 3) cooling after the surface is "quenched" to room temperature, (*i.e.* the surface temperature is equal to room temperature). The first and third cases provide two extreme conditions: infinitely large thermal conductivity (slow cooling) and infinitely large convection (or radiation) coefficient (constant surface temperature).

PART ONE — HEAT TRANSFER

To solve the problem analytically, we use the following assumptions: 1) Heat convection and radiation are assumed to take place only in the thickness direction. Any heat transfer around the edge is neglected. This assumption reduces the analysis to a one-dimensional problem. 2) Although the thermal conductivity, k, mass density, ρ, and the specific heat, C_p, all are functions of temperature, the ratio $k/\rho C_p$ is assumed to be temperature independent. 3) Linearization of thermal boundary conditions is assumed to be acceptable.

The governing differential equation for heat conduction without any inside heat source (Fourier equation) is [7]

$$\frac{\partial}{\partial z}[\,k(T)\frac{\partial T}{\partial z}] = \rho(T)C_p(T)\frac{\partial T}{\partial t}$$

or when the ratio $k/\rho C_p$ is independent of temperature

$$\alpha\frac{\partial^2 T}{\partial z^2} = \frac{\partial T}{\partial t} \tag{1}$$

where $\alpha = k/\rho C_p$. The analysis of slowly cooled laminates does not involve any heat conduction analysis. The analyses of laminates cooled by convection and radiation or by quenching both use Eq. (1), but require different boundary conditions.

The heat convection and radiation boundary condition has the form

$$-k\frac{\partial T(d,t)}{\partial z} = I_r + I_c \tag{2}$$

where d is the half thickness of the plate, I_r and I_c are the surface energy losses due to radiation and convection, respectively, which are normally assumed to be

$$I_r = \sigma\varepsilon[T_{su}^4 - T^4(d,t)] \qquad \text{(Stefan-Boltzmann law)} \tag{3}$$

$$I_c = h_c[T_r - T(d,t)] \qquad \text{(Newton cooling law)} \tag{4}$$

where h_c is the convection coefficient; T_r is the air recovering temperature; σ is the Stefan-Boltzmann constant; ε is the surface emissivity of a "gray body" (instead of "black body"); and T_{su} is the temperature of an object surrounding the composite plate and receives the radiated heat. Because h_c and T_r are very complex functions of surface temperature, T(d,t) [5], both the convection and radiation parts of this boundary condition are nonlinear. To solve the problem analytically, we have to "linearize" the boundary condition. We linearize the convection part by assuming h_c to be temperature independent and letting T_r equal room temperature — T_0. We linearize the radiation part by letting $T_{su} = T_0$ and using the following simplification

$$I_r = \sigma\varepsilon[T_0^4 - T^4(d,t)] = \sigma\varepsilon[T_0^2 + T^2(d,t)][T_0 + T(d,t)][T_0 - T(d,t)] = h_r[T_0 - T(d,t)] \tag{5}$$

where $h_r = \sigma\varepsilon[T_0^2 + T^2(d,t)][T_0 + T(d,t)]$ is assumed to be approximately independent of temperature [8,9]. Further we let $T^*(z,t) = T(z,t) - T_0$ and consequently the boundary condition is not only linear but also homogeneous:

$$\frac{\partial T^*(d,t)}{\partial z} = \left(\frac{h_c + h_r}{k}\right) T^*(d,t) = \beta T^*(d,t) \tag{6}$$

where $\beta = (h_c + h_r)/k$. Together with the boundary condition at the symmetric axis

$$\frac{\partial T(0,t)}{\partial z} = \frac{\partial T^*(0,t)}{\partial z} = 0 \tag{7}$$

and the initial conditions

$$T(z,0) = T_{sf} \qquad \text{and} \qquad T^*(z,0) = T_{sf} - T_0 \tag{8}$$

where T_{sf} is the stress-free temperature, we can solve Eq. (1) by the method of separation of variables.

The general solution takes the form

$$T^*(z,t) = e^{-\lambda^2 \alpha t}(A_1 \sin\lambda z + A_2 \cos\lambda z) \tag{9}$$

Equation (7) yields $A_1 = 0$ and Eq. (6) gives

$$\lambda \tan\lambda d = \beta$$

This is a characteristic equation having an infinite number of roots — λ_n. Because the differential equation (Eq. (1)) is linear, any possible linear combination of the solutions is also a solution. The general solution then becomes

$$T^*(z,t) = \sum_{n=1}^{\infty} a_n e^{-\lambda_n^2 \alpha t} \cos\lambda_n z \tag{10}$$

The remaining task is to determine a_n by the initial condition (Eq. (8)). This task can be done analytically only if $\cos \lambda_n z$ is an orthogonal series, which happens when either $\cos \lambda_n$ or $\sin \lambda_n$ is zero for all n (*i.e.* is $\lambda_n = n\pi$ or $\lambda_n = n\pi + \pi/2$) and the problem has the appropriate boundary conditions. Because β is positive, we apprehend that $\lambda_n \approx (n-1)\pi$ for n=2, 3, 4, ... and the larger the n, the closer they are. Therefore Eq. (10) can be approximately treated as an orthogonal series. By normalizing the half thickness of plate d to unity and using one of the criteria for the orthogonality condition in Ref. [8], we obtain

$$a_n = \frac{1}{b_n}\int_0^d (T_{sf} - T_0)\cos\lambda_n z \, dz \tag{11}$$

where

$$b_n = \int_0^d \cos^2\lambda_n z \, dz$$

Substitution of b_n into Eq. (11) gives

$$a_n = \frac{4(T_{sf} - T_0)\sin\lambda_n d}{2\lambda_n d + \sin 2\lambda_n d} \tag{12}$$

and finally, we have

$$T(z,t) = T_0 + (T_{sf} - T_0)\sum_{n=1}^{\infty} \frac{4\sin\lambda_n d}{2\lambda_n d + \sin 2\lambda_n d} \cos\lambda_n z \, e^{-\lambda_n^2 \alpha t} \tag{13}$$

Because the expression for a_n is approximate, we found it necessary to include more than 100 terms in Eq. (13) to get convergence to the correct answer.

For quenched laminates or laminates with a constant temperature surface, the boundary condition is simply

$$T^*(d,t) = 0$$

The general solution (Eq. (9)), symmetry condition (Eq. (7)) and initial condition (Eq. (8)) are still valid. The above boundary condition reveals

$$\cos\lambda d = 0$$

which results in

$$\lambda_n = n\pi + \pi/2 \qquad n=1, 2, 3, ...$$

We can evaluate a_n by the same procedure used for convection and radiation cooling except that λ_n now defines an exact orthogonal series and the corresponding expression for a_n is therefore exact instead of approximate. The final expression of temperature distribution in quenched laminates is the same as Eq. (13) except the values of λ_n are changed.

PART TWO — THERMALLY-INDUCED RESIDUAL STRESSES

The material used in the present study is ICI PEEK/Hercules AS4 carbon fiber prepreg whose thermal expansion coefficient and Young's modulus were provided by ICI Composites. Due to the fiber dominant nature and the temperature insensitivity of the mechanical and thermal properties of carbon fibers, the mechanical and thermal properties in the fiber direction of composites can be assumed to be temperature independent. Experiments show that for this material only a 2.5% error will be introduced by using this assumption [10]. In contrast, the transverse mechanical and thermal properties are temperature dependent. ICI composites supplied experimental results for transverse mechanical and thermal properties from room temperature to the stress-free temperature.

In the analysis of thermally-induced residual stresses in a cross-ply laminate, so-called Classical Lamination Theory is used. Consider a flat plate of uniform thickness with an available temperature distribution T(z,t). Classical Lamination Theory gives [11]:

$$\{\sigma\} = [Q](\{\varepsilon\} - \{\alpha\}\Delta T(z,t)) \tag{14}$$

$$\{\varepsilon\} = \{\varepsilon_0\} + z\{\kappa\}$$

where [Q] is the stiffness matrix, $\{\varepsilon_0\}$ are the strains in the mid-plane of the plate, $\{\alpha\}$ are the thermal expansion coefficients and $\{\kappa\}$ are the plate curvatures. Because we deal with symmetric laminates only, their curvatures due to temperature change are zero and therefore

$$\{\sigma\} = [Q](\{\varepsilon_0\} - \{\alpha\}\Delta T(z,t)) \tag{15}$$

The residual stresses are zero at the stress-free temperature and start to build up as the laminate cools below this temperature. We assume that below the stress-free temperature the plate is solidified and the displacement along the thickness direction is uniform. Eq. (15) is a general expression for a

temperature-independent material. Because the material we investigate is strongly temperature dependent, however, Eq. (15) has to be modified. If the temperature has an infinitesimal change from T to T+ΔT, the stresses change by

$$\{\Delta\sigma\} = [Q(T)]\{\Delta\varepsilon_0\} - [Q(T)]\{\alpha(T)\}\Delta T(z,t) \tag{16}$$

where [Q(T)] and {α(T)} are the stiffness matrix and thermal expansion coefficient at temperature T. We slice the laminate into *m* thin layers and assume that each layer is thin enough to ignore the gradients of temperature as well as stress and strain. Because there are no applied forces, the equilibrium equation is taken to be

$$\int_D \sigma_p \, dz = 0$$

where p = x or y and D is the thickness domain. For a discretized thickness domain we have

$$\sum_{i=1}^{m} \Delta\sigma_i \Delta z_i = 0 \tag{17}$$

With the substitution of Eq. (16) into Eq. (17) and taking Δz_i as a constant we easily obtain

$$\Sigma[Q_{11i}(\Delta\varepsilon_x - \alpha_{xi}\Delta T) + Q_{12i}(\Delta\varepsilon_y - \alpha_{yi}\Delta T)] = 0$$

$$\Sigma[Q_{12i}(\Delta\varepsilon_x - \alpha_{xi}\Delta T) + Q_{22i}(\Delta\varepsilon_y - \alpha_{yi}\Delta T)] = 0$$

where Q_{11i}, Q_{12i}, α_{xi}, *etc.* are elements of the stiffness matrix and of the thermal expansion coefficient vector at temperature T; and $\Delta\varepsilon_x$ and $\Delta\varepsilon_y$ are variations of total strains in x and y directions, which are z independent, due to temperature variation from T to T + ΔT. These two equations lead to the expressions for $\Delta\varepsilon_x$ and $\Delta\varepsilon_y$

$$\Delta\varepsilon_x = \frac{(\Sigma Q_{11i}\alpha_{xi}\Delta T + \Sigma Q_{12i}\alpha_{yi}\Delta T)\Sigma Q_{22i} - (\Sigma Q_{12i}\alpha_{xi}\Delta T + \Sigma Q_{22i}\alpha_{yi}\Delta T)\Sigma Q_{12i}}{\Sigma Q_{11i}\,\Sigma Q_{22i} - (\Sigma Q_{12i})^2}$$

$$\Delta\varepsilon_y = \frac{(\Sigma Q_{12i}\alpha_{xi}\Delta T + \Sigma Q_{22i}\alpha_{yi}\Delta T)\Sigma Q_{11i} - (\Sigma Q_{11i}\alpha_{xi}\Delta T + \Sigma Q_{12i}\alpha_{yi}\Delta T)\Sigma Q_{12i}}{\Sigma Q_{11i}\,\Sigma Q_{22i} - (\Sigma Q_{12i})^2}$$

and eventually two expressions for the residual stress variation of each slice:

$$\Delta\sigma_{xi} = Q_{11i}(\Delta\varepsilon_x - \alpha_{xi}\Delta T) + Q_{12i}(\Delta\varepsilon_y - \alpha_{yi}\Delta T)$$

$$\Delta\sigma_{yi} = Q_{12i}(\Delta\varepsilon_x - \alpha_{xi}\Delta T) + Q_{22i}(\Delta\varepsilon_y - \alpha_{yi}\Delta T)$$

Finally the total residual stresses for each slice can be determined by summing each variation of stress in the temperature (or time) domain

$$\sigma_{xi} = \Sigma\, \Delta\sigma_{xi}$$

$$\sigma_{yi} = \Sigma\, \Delta\sigma_{yi}$$

NUMERICAL STUDY AND CONCLUSIONS

According to data provided by ICI Composites, we selected thermal conductivity k = 0.25 W/m-°K, specific heat capacity C_p = 1.5 kJ/kg-°K = 0.4167 W-hr/kg-°K, and average density ρ = 1.3 g/cm^3. From other sources we selected the convective heat transfer coefficient h_c = 2.5 Btu/hr ft^2-°F = 14.186 W/m^2-°K [7], Stefan-Boltzmann constant $\sigma = 0.1714 \times 10^{-8}$ Btu/hr-ft^2-°R^4 $= 5.669 \times 10^{-4}$ W/m^2-°K^4 [7], and surface emissivity ε = 0.92 [5].

Figures 1 and 2 illustrate the distributions of x-axis residual stresses for thin laminates $[0_2/90_2]_s$ and $[90_2/0_2]_s$. Figures 3 and 4 show the results for thick laminates $[0_{90}/90_5]_s$ and $[90_5/0_{90}]_s$ (about one inch thick). We draw the following conclusions:

(1) For thin laminates the slow cooling results are close to the convection and radiation results. This implies that the assumption of a uniform temperature distribution is adequate for thin laminates. For thick laminates the convection and radiation results are between those of slow cooling and quenching results, which indicates that an assumption of uniform temperature distribution is not adequate. An accurate estimation of the non-uniform residual stresses in thick laminates must use an analysis that accounts for heat conduction similar to the one in this paper.

(2) The residual stresses in quenched laminates, as well as in thick laminates under convective and radiative cooling, always have a high gradient at the laminate surface. The magnitude of stress variation in this area remains unchanged regardless of the laminate thickness. The high normal residua stress gradient caused by nonuniform cooling will likely produce a high shear stress gradient, which might cause local delamination.

(3) Beyond this high gradient stress area the residual stresses within each ply group remain nearly uniform. Thus, the residual stresses away from this area in thick laminates will be nearly unaffected by processing conditions.

COMMENTS

The processing conditions affect the cooling temperature distribution and may consequently cause nonuniform residual stresses. The effects of processing conditions are strongest near the surfaces of laminate where the residual stresses can differ significantly from those calculated by a simple laminated plate theory that assumes a uniform temperature distribution during cooling. At the center of laminates, a simple uniform temperature distribution gives a good estimate of the ply residual stresses.

Numerical results support the claim that the residual stresses in "quenched" laminates and in slowly cooled laminates provide upper and lower bounds to the residual stresses. Either one may provide the upper bound somewhere and the lower bound somewhere else. The results for convection and radiation, however, will definitely be bounded by the upper and lower bounds. In real applications, it will be very hard, if not impossible, to precisely describe the cooling boundary conditions in processing. If the upper and lower bounds are given, it will help the designer to have an estimate on the level of the residual stresses.

We believe that below the stress-free temperature of PEEK composites that the plate is solidified and is also fully crystalized [6]. Any significant crystallization happening below the stress-free temperature might cause volume reduction and result in extra residual stresses. We also assumed that viscoelastic behavior of PEEK material does not significantly influence the residual stresses. If a great amount of time is spent above the glass transition temperature, it is possible that stress-relaxation will reduce the level of residual stresses. Most residual stresses form, however, when the matrix is stiff and below the glass transition temperature. At these lower temperatures, stress relaxation effects are probably minimal.

ACKNOWLEDGMENTS

This work was supported in part by a contract from NASA Langley Research Center (NAS1-18833) monitored by Dr. John Crews, in part by a gift from ICI Advanced Composites monitored by Dr. J. A. Barnes, and in part by a gift from the Fibers Department of E. I. duPont deNemours & Company monitored by Dr. Alan R. Wedgewood.

REFERENCES

1. Jeronimidis, G., and Parkyn, A. T., "Residual Stresses in Carbon Fiber-Thermoplastic Matrix Laminates," Journal of Composite Materials, Vol. 22, 1988, pp. 401-415.
2. Hahn, H. T., "Residual Stresses in Polymer Matrix Composite Laminates," Journal of Composite Materials, Vol. 10, 1976, pp. 266-278.
3. Hussein, R. et al, "Thermal Stresses in Sandwich Plates," Journal of Thermal Stresses, Vol. 12, 1989, pp. 333-349.
4. Griffis, C. A., et al, "Degradation in Strength of Laminated Composites Subjected to Intense Heating and Mechanical Loading," Journal of Composite Materials, Vol. 20, 1986, pp. 216-220.
5. Chen, J. K., et al, "Failure Analysis of a Graphite/Epoxy Laminate Subjected to Combined Thermal and Mechanical Loading," Journal of Composite Materials, Vol. 19, 1985, pp. 408-416.
6. Nairn, J. A., and Zoller, P., "Residual Thermal Stresses in Semicrystalline Thermoplastic Matrix Composites," Fifth International Conference on Composite Materials (ICCM-V) July, 1985.
7. Sucec, J., Heat Transfer, WM. C. BROWN Publishers, Dubuque, Iowa, 1985.
8. Mayers, G. E., Analytical Methods in Conduction Heat Transfer, McGraw-Hill Book Company, New York, 1971.
9. Biot, M. A., Variational Principles in Heat Transfer, Oxford University Press, London, 1970.
10. J. A. Barnes, I. J. Simms, G. J. Jackson, D. Jackson, G. Wostenholm, and B. Yates, "Thermal Expansion Behaviour of Thermoplastic Composites," ASME Winter Meeting, Dallas, Texas, November 25-30, 1990.
11. Tauchert, T. R., "Thermal Stresses in Plates — Statical Problem," Chapter 2 of Thermal Stresses I, R. B Hetnarski Ed., North-Holland, Amsterdam, 1986.

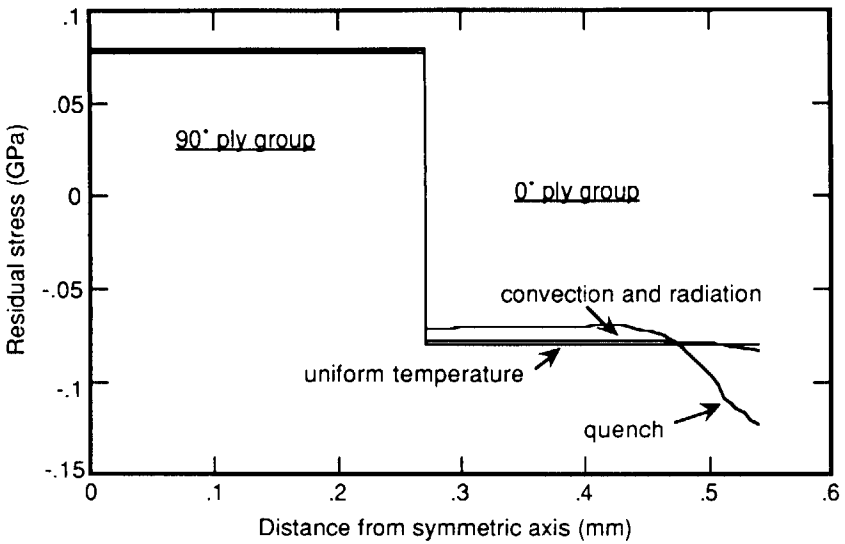

Figure 1: The distributions of x-axis residual stresses in a $[0_2/90_2]_S$ laminate cooled under uniform temperature distribution (slow cooling), by convection and radiation, and by quenching to room temperature.

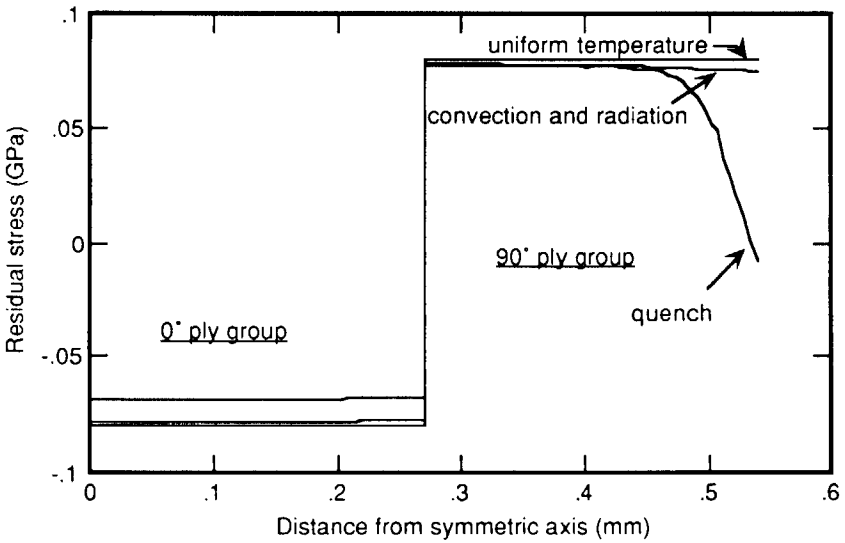

Figure 2: The distributions of x-axis residual stresses in a $[90_2/0_2]_S$ laminate cooled under uniform temperature distribution (slow cooling), by convection and radiation, and by quenching to room temperature.

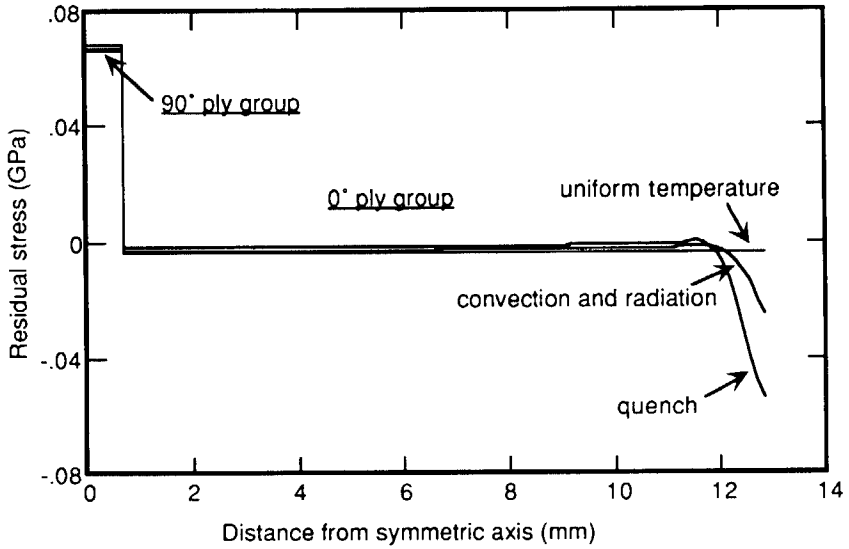

Figure 3: The distributions of x-axis residual stresses in a $[0_{90}/90_5]_S$ laminate cooled under uniform temperature distribution (slow cooling), by convection and radiation, and by quenching to room temperature.

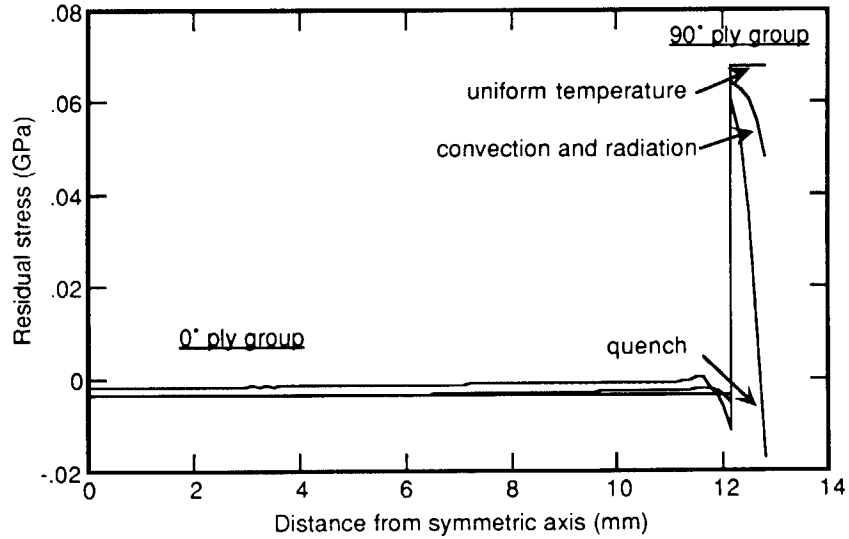

Figure 4: The distributions of x-axis residual stresses in a $[90_5/0_{90}]_S$ laminate cooled under uniform temperature distribution (slow cooling), by convection and radiation, and by quenching to room temperature

Advanced Fabrication Processes for Thick Composite Submarine Structure

James J. Kelly
DARPA

George Leon
GD/Electric Boat

Diana Holdinghausen
McDonnell Aircraft Corporation

THIS PAGE INTENTIONALLY BLANK

LOW - COST DESIGN AND FABRICATION OF COMPOSITE SHIP STRUCTURES

Milton O. Critchfield and Thomas D. Judy
David Taylor Model Basin
Carderock Division, Naval Surface Warfare Center
Bethesda, Maryland

omit

SUMMARY

The U.S. Navy has demonstrated a low-cost resin transfer molding process for the fabrication of high performance composite ship structures including monocoque, single skin stiffened, and sandwich configurations. The resulting mechanical properties for the structures are competitive with properties achieved using wet lay-up or prepreg and autoclave cure. Composite design concepts and prototypes have been developed for composite deckhouse, mast, and foundation structures and fabricated using this process. Prototype structural performance has been successfully demonstrated under dynamic load requirements including air blast and shock. The paper also discusses some recent successful experience with the repair of a thick glass-reinforced plastic sonar dome using this process. Some potential near-term applications of the fabrication process for composite ship structures are identified.

INTRODUCTION

The naval ship structure community is pursuing the challenge of improving the structural performance of naval ships while reducing ship construction and life cycle maintenance costs. In addition to reducing structural weight, efforts are being made to reduce fatigue cracking, corrosion, and noise transmission, increase fragmentation and shock resistance, and improve fire containment. Composite structures offer the clear potential for achieving improvements in all of these areas. Some structural applications where these improvements are under development or consideration are shown in figures 1 and 2.

In order to exploit the advantages of composites for these applications, innovative design concepts, and low-cost processes to fabricate high quality composite structures are needed. In particular, a fabrication process is needed that approaches the cost of glass reinforced plastic (GRP) marine construction (reference 1) but results in the quality of typical aerospace construction. Furthermore, a versatile process is needed that allows for the fabrication of a range of composite structures from thick monocoque to single skin stiffened and sandwich construction using a variety of resins and fiber reinforcements.

The U.S. Navy has been successful in demonstrating a low-cost vacuum resin transfer molding (RTM) process having the capability and versatility just described. The process has been used to fabricate composite deckhouse structural modules, a one - half scale composite mast, and a one - half scale composite foundation. This paper will describe the U. S. Navy's experience with this process and with the

1456 - 1459

design, fabrication and testing of these composite prototypes. Some limited experience with the use of the vacuum RTM process for repair will also be covered along with some potential near-term applications of this process for the fabrication of affordable high quality composite ship structures.

LOW-COST FABRICATION OPTIONS

A number of low-cost options are available for the fabrication of composite ship structures. The most promising of these are resin transfer molding, pultrusion and filament winding. The particular method chosen for a given application depends upon the requirements of the application such as structure or component size, geometry, and desired mechanical properties. Some typical ship structural components would include GRP beams, panels of monocoque, stiffened and sandwich construction, and rectangular and cylindrical modules of similar construction.

Although pultrusion is an attractive process for producing low - cost beams and panels having a uniform or prismatic cross-section, the process is not able to deal with non-uniform or tapered members. While filament winding does not have this limitation, it is generally not able to handle complex structural geometries and the incorporation of stiffeners.

RTM methods, on the other hand, have the versatility to deal with a variety of structural configurations. As an example, they are able to accommodate tapered beams and panels and three dimensional structures having rather complex geometries. Reference 2 is an excellent relatively recent article describing the status of development of RTM methods for advanced composites.

In general, RTM methods seem to fall into one of the three following categories:

- Conventional RTM
- Vacuum Assisted RTM
- Vacuum RTM

With the conventional RTM method, dry fiber reinforcement or preform is loaded into a split mold (usually female and male), the mold is clamped together and resin is injected under pressure. This process is used for the manufacture of such medium to large size parts as car bodies, bus shelters, hatch covers, and shower enclosures (reference 3). The term vacuum assisted RTM has been used in industry to refer to two types of RTM processes, one in which the vacuum assists the process of resin injection 'under pressure', and the second where the resin is injected 'under vacuum' alone. For example, vacuum assistance is often used with conventional RTM to remove air and volatiles from the part during resin injection under pressure. Vacuum assisted has also been used to describe several processes developed in Europe which utilize only a vacuum and no pressure to transfer the resin. One of these has been used to fabricate a 22 m landing craft (reference 4). The term Vacuum RTM has been introduced in this paper to try to eliminate the confusion and to describe processes where a full vacuum, without pressure, is used to consolidate the dry fiber reinforcement and to inject resin into the structure.

Vacuum RTM, as defined here, is apparently employed at relatively few companies worldwide. Some of the companies either investigating or using vacuum and vacuum assisted RTM processes are listed in Table 1 along with their applications to date. It should be noted that these applications involve the use of an open mold, either male or female, or a closed or split mold. The open mold approach is less expensive because it minimizes the amount of tooling required.It may be used when only a single mold surface is required.

The U.S. Navy has been very successful in evaluating and demonstrating a low-cost vacuum RTM process for the fabrication of composite deckhouse, mast, and foundation structures. The particular vacuum RTM process evaluated is the Seemann Composites Injection Molding Process (SCRIMP). The SCRIMP process uses a single open mold and a patented resin distribution system, including a patented distribution medium, for achieving aerospace quality composites. The patented process has resulted in high fiber content, approximately 70% by weight for glass, and very low void content (<1%). Resultant mechanical properties are considerably greater than properties achieved with standard 50 to 60 % glass content panels and are competitive with properties obtained using wet lay-up or prepreg and autoclave cure procedures (See Table 2).

PANEL FABRICATION USING 'SCRIMP'

The first panel fabricated using the SCRIMP process for the U.S. Navy was a 8'x16' hat-stiffened deckhouse panel in figure 3. At the time of its fabrication in 1989 the panel was apparently the largest high performance composite panel fabricated using an RTM process in North America. The SCRIMP process was used to demonstrate a more affordable alternative to the wet lay-up autoclave cure process utilized to fabricate the original panel. The deckhouse panel in figure 3 involves tapered stiffeners, 6" deep and 6" wide at midspan, with skin thickness ranging from 0.5" between stiffeners at midspan to 0.75" at the panel edges. Stiffener flange and web thicknesses varied from 0.2" at midspan to 0.4" at the stiffener extremities. Although the original autoclave panel was fabricated using E- glass and isophthalic polyester resin, the SCRIMP fabricated panel utilized a vinyl ester resin to improve the toughness of the panel under dynamic loading and to facilitate the SCRIMP process.

Figure 4 shows a schematic layout for the SCRIMP process for a segment of the hat stiffened panel. The basic steps in the SCRIMP process for the hat stiffened panel are summarized below.

1. The dry reinforcement preform, including the stiffener cores,are laid up on the rigid mold.
2. The preform is covered by a peel ply, distribution medium, and a vacuum bag in that order.
3. A full vacuum is drawn to consolidate the panel and inject the resin.
4. Resin is allowed to flow into the panel until full wetting occurs.
5. The panel is allowed to cure for approximately 8 hours at room

temperature.

6. The panel is oven post-cured at an average temperature of 140 degrees F for 8 hours.

The most labor intensive part of the process is the laying up of the dry preform for the panel. The base skin (0.32") of the panel, under the stiffener cores, was laid up first out of 8 plies of 50 oz, twill weave fabric, woven by Seemann Composites. Five plies of 50 oz twill weave were then draped over the stiffener cores. Five blocks of 24 oz woven roving at 45^0 and 90^0 were feathered into the 50 oz twill weave over the taper region of the stiffeners. The last two columns of Table 2 compare the mechanical properties achieved for the SCRIMP panel with those obtained for the autoclave panel. The properties for the two panels are seen to be comparable with the interlaminar shear strength seen to be clearly superior as expected for the viny ester over the polyester panel.

In addition to the hat stiffened panels, a series of 4'x4' and 8'x16' composite sandwich panels were also fabricated using the SCRIMP process and a variety of resin and core materials. The above process, with some variations, was used for all of these panels.

Sandwich panels with foam and balsa cores, up to 4.0 " thick, were laid up and resin injected in one step. The process took advantage of narrow vertical slits in the balsa core product for transferring resin from the upper to lower skin of the panel. Table 2 compares the mechanical properties of the 70 % glass content skins (see columns 2 and 3), for some of these sandwich panels, with corresponding 50% glass content skin properties (column 1) resulting from panels produced using standard wet lay-up boat-building methods. The advantage of the SCRIMP process in providing 70% glass content and significantly better mechanical properties is evident.

DESIGN CONCEPTS AND PROTOTYPE DEMONSTRATIONS

The U.S. Navy has successfully developed and demonstrated composite design concepts for a number of ship structural applications including deckhouses, masts, and foundations. Each of these composite prototypes were fabricated using the SCRIMP process and will be taken up next in the paper.

Composite Deckhouse

Composites offer a number of advantages for deckhouse application, the principal ones being reduced weight by up to 45%, elimination of corrosion and fatigue cracking, and the capacity for fire containment.

Composite deckhouses must be designed for a number of loadings including air blast, hydrostatic pressure, and hull- deckhouse interaction loads. Since air blast is the governing load condition, extensive dynamic tests have been conducted to evaluate the structural resistance of composite beams, panels, and modules to air blast loading.

The currently favored approach for the shipyard construction of composite deckhouses is the prefabrication of large high quality composite panels and their attachment to an erected supporting steel

framework as indicated in figure 5 (reference 5). Since these panels could be fabricated off-line at a vendor or using a licensed process in a shipyard, the opportunity exists to fabricate the composite panels with extremely low void content and significantly higher mechanical properties than normally achieved with traditional wet lay-up room temperature cure methods used to fabricate large GRP structures such as naval minesweepers and minehunters. Some of current bolted - bonded joint configurations for the connection of composite panels to the steel framework of a deckhouse are shown in figure 6.

Two composite panel design concepts, single skin hat stiffened and sandwich core panels, have been developed for deckhouse and superstructure construction. The use of monocoque GRP panels on closely-spaced steel framing, a solution under development by the British Navy(reference 6), has not been pursued because it is significantly heavier than the use of single skin stiffened and sandwich panels on more widely-spaced framing.

Single Skin Construction

GRP single skin stiffened construction was initially pursued for deckhouse structure because it involved less risks than sandwich construction in areas such as fatigue and shock resistance, environmental effects and general ruggedness. A tapered hat stiffened panel concept was developed as a basic building block for deckhouse construction. The stiffeners are tapered to make them peel - resistant under loading, to minimize panel weight, and to simplify the joining of panels to steel frames. Joining is facilitated because of the single skin thickness around the perimeter of the panel. The fabrication of the hat stiffened panels using the SCRIMP process was discussed in detail earlier.

In order to evaluate the structural performance of the hat stiffened concept under air blast loading, an 8'x15' panel was fabricated using a wet lay- up autoclave cure procedure. Panels were also fabricated using the SCRIMP process and used in the construction of a 16'x8'x8' module as shown in figure 7(a). The module was assembled using GRP connection angles since GRP was initially favored over steel for the supporting framework of deckhouses and superstructures. Figure 7(b) shows a photograph of the bolted- bonded joint details for this module. Many bolts were used to provide a conservative design.

The module was successfully air blast tested at the White Sands Missile Range under the MISERS GOLD and DISTANT IMAGE events in 1989 and 1991. In the first test, at an equivalent static pressure of approximately 30 psi, the front of the module deflected approximately 2 inches and half moon shaped delaminations appeared along the inside bottom of the front panel where the GRP panel was bolted to a rather rigid steel coaming. The extent of delamination damage (figure 8) grew considerably in the second test, at an equivalent static pressure of a little over 50 psi (maximum front panel deflection of 5.6 inches), but the damage was still acceptable since no rupture of the module panels occurred. The acceptable damage to the module, under the severe dynamic loading, demonstrates the superior toughness of the structure resulting from the SCRIMP process and the vinyl ester resin even at high glass contents (approximately 70%).

Additional air blast tests have been conducted on one-half scale GRP hat stiffened panels to evaluate and screen a variety of bolted- bonded joint details for use with these panels. These panels, fabricated using the SCRIMP process, were dynamically tested in a blast tube at the Defence Research Establishment Suffield (DRES), Alberta under a collaborative effort with the Canadian Navy. These tests explored the options of greater bolt spacings, the use of countersunk bolts, and the performance of steel versus GRP connection angles. This test series resulted in the streamlined bolted- bonded detail in figure 7 (c) which was adopted in the construction of a composite sandwich module to be discussed next. Figure 9 shows the delamination damage observed after the blast tube test of one of the half scale panels. It was found to be similar to the delamination shown in figure 8 at the bottom of the hat stiffened module for a similar pressure.

This paper has not addressed the integration of electromagnetic issues such as electromagnetic shielding and lightning strike protection into the design. The effectiveness of the SCRIMP process in fabricating composite deckhouse panels with these features must still be demonstrated.

Sandwich Construction

Sandwich construction offers a number of advantages over single skin stiffened for marine as well as aerospace applications. Some of the particular advantages for naval deckhouses are increased weight reduction over single skin stiffened of 10% or more, an inherent thermal insulation capability, and a flat surface on panel interiors for ease of outfitting.

In order to select the most promising sandwich options for deckhouse structure, the dynamic structural performance of a variety of composite sandwich panels were air blast tested and evaluated in a blast tube at DRES under a joint effort with the Canadian Navy. Various panel geometries (uniform and tapered), cores (balsa, poly vinyl chloride, and polymethacrylimide), resins (vinyl ester, polyester, and phenolic) and glass contents (50% and 70%) were evaluated in the test series. As a result of these tests, a tapered panel fabricated using the SCRIMP process with a balsa core and vinyl ester resin was selected. This panel showed no visible signs of delamination even after air blast testing to a maximum equivalent static pressure of 72 psi.

Following the successful test of the tapered vinyl ester panel, a fire hardened concept was developed by introducing a structural skin at mid-depth in the balsa core panel. This panel withstood a pressure of 155 psi without rupture. The fire hardened tapered panel was successfully manufactured using the SCRIMP process in a two step process. The lower half of the panel was first fabricated by 'scrimping' the middle skin and bottom skin to the lower balsa layer. The upper skin and upper balsa layer was then 'scrimped' to the lower layer.

The above process was used to fabricate the 16'x8' and 8'x8' fire hardened panels for a 16'x8'x8' sandwich module. These panels were bolted and bonded to an erected steel framework comprised of steel angles. The particular epoxy bonding adhesive selected provided good toughness and elongation characteristics under dynamic loading. The module was air blast tested at White Sands with an equivalent static

pressure of approximately 30 psi on the front of the module.

This resulted in a maximum deflection of 4.8 inches of the front of the module and some acceptable delamination in the panel taper around the perimeter of the front panel. The extent of delamination at the inside bottom of the front panel was probably minimized by allowing the steel coaming to deform plastically under loading. A comparison of overall structural performance of the GRP stiffened and sandwich module is given in Table 3.

A comparison of weight and costs to fabricate the individual panels for the stiffened and sandwich modules and to construct these modules is given in Table 4. It should be noted that the fire - hardened sandwich panels in Table 4 were more expensive to fabricate than non fire - hardened panels. Also, these costs are associated with the fabrication of one-of-a-kind prototypes and involve significant engineering and manufacturing development costs. A substantial reduction in costs approaching 50 % is expected for full production. As an example, it is expected that the cost to fabricate the stiffened panels will drop from $9.40 per pound for the prototype to $5 to $8 per pound in production.

Composite Mast

The weight and height of masts have a significant impact on the stability and seakeeping characteristics of naval ships. Composite masts are therefore a most attractive option for either upgrading the stability of existing ships through backfit applications or providing a greater topside weight growth margin in the construction of new ships. Design studies have shown that a composite mast can be expected to save from 20% to 50% over a conventional metallic mast. In addition to the weight reduction benefits, the use of composites would also eliminate corrosion, improve fatigue performance, and improve the performance of mast sensors by reducing electrical blockage over that of metallic masts.

In order to demonstrate the feasibility of a composite mast for naval combatants, a one- half scale, 36 foot tall, prototype mast(see figure 10) was designed, fabricated and tested under a Cooperative Research and Development Agreement (CRDA) between the David Taylor Research Center (DTRC) and Ingalls Shipbuilding. In developing the prototype mast, the external configuration and geometry of the existing DDG- 51 mast was adopted as a baseline. A weight reduction of 20% was realized against this aluminum baseline design.

The mast structure and elements were designed to meet the vibration requirements (bending frequency > 3.5 hz.), to have a factor of safety of 1.0 for air blast loads, and to match the ballistic performance of the existing aluminum mast. A hybrid material system of S-2 glass and carbon in a vinyl ester matrix was selected for the main trunk of the mast; S-2 glass was chosen to maximize the ballistic performance and carbon in a +/- 45 degree layup to provide sufficient torsional stiffness. S-2 glass was used for the other elements of the mast.

The composite mast model was constructed by fabricating the main individual elements of the mast, that is, the trunk, two yardarms, and two stays, using the SCRIMP process. These large elements were then shipped to White Sands where they were bolted together and the mast

erected for the DISTANT IMAGE air blast test in June 1991. In the interest of enhancing producibility, commercially available pultruded GRP struts were used to support the yardarms from the trunk and aluminum connection details were used at the extremities of the struts.

Figure 11 illustrates the materials, geometry and details for the fabrication of the main trunk of the mast. The main trunk, 28.5 feet long with a square cross section measuring 27 inches on a side, was fabricated in two halves. Each half of the trunk was a large angle member that was laid-up using dry E-glass and carbon fabric in a female mold and then 'scrimped' in one step. E- glass was used because of the unavailability of S-2 glass to meet the fabrication schedule. An adjustable female mold was used to allow for the effect of anticipated shrinkage on the corner angles. The carbon fabric was imbedded at mid depth in the E-glass laminate to minimize the release of carbon fiber in an explosion. The SCRIMP process was also used to fabricate the corner elements. The entire trunk was then assembled together using limited bolts and an epoxy adhesive that proved effective for the deckhouse module. A similar process was used to fabricate the yardarms and aft legs or stays whose cross-sections are shown in figure 12. The composite mast prototype was fabricated for a cost of $42 per pound. Since there was considerable engineering and manufacturing development included in this cost, it is felt that composite masts could be produced in full- scale production at a cost of $20 to $30 per pound.

The one-half scale mast was tested at the DISTANT IMAGE event to a substantial air blast loading which produced an overall deflection of approximately 6 inches at the top of the mast. Although the dynamic high speed photos showed the mast trunk, and especially the yardarms, to be clearly vibrating from the effects of the air blast, virtually no damage occurred. A careful examination of the mast exterior revealed only one small delamination 2 to 3 inches in diameter on a large connecting bracket for the mast platform. Close agreement was obtained between the measured overall bending frequency for the mast (6.7 hz- one -half scale; 3.35 hz - full scale) and the design value (3.5 hz).

Composite Foundations

The use of composite materials for foundation structures offers many potential advantages over current steel structures. Weight reductions of over 50% are possible in some applications. Even more important in many naval applications is the potential for improving the noise transmission characteristics of machinery/ equipment foundations. Additional benefits include the mitigation of shock loads to the supported equipment, improved corrosion resistance, and reduced magnetic signature.

In order to demonstrate the structural feasibility of composite materials in foundation structures, a one-half scale pump foundation was designed, fabricated, and tested under an exploratory development program for submarine structures. The baseline selected for this demonstration was a fresh water pump foundation. This foundation is attached to the upper level deck in an engine room and supports a bedplate, pump, and motor. In this demonstration, a composite foundation was designed to match the existing geometrical constraints. A weight reduction of 40% was obtained relative to the existing steel

structure. Additional savings could have been achieved by integrating composites into the initial system design instead of replacing an existing steel design.

The current steel foundation, shown in figure 13, is fabricated from welded high strength (HY-80) steel plate. A one-half scale composite model of the foundation was developed and analyzed using the finite element computer program ABAQUS. The idealized composite structure consists of 150 elements, 1160 nodes and 3500 degrees of freedom. The governing loads for foundation design and finite element analysis are derived from the shock requirements of MIL-S-901D. Stresses resulting from an equivalent static load of 40,000 pounds are presented in figure 14 to show the distribution of stresses in the composite model for the athwartship load case.

In selecting a vendor to fabricate the foundation model, cost was a major consideration. Rough cost estimates were obtained from a number of vendors representing different composite fabrication processes. The SCRIMP process (described earlier) was selected because cost estimates were 50% less than other methods. An epoxy resin was selected for the foundation based on strength and shrinkage considerations. The areas in the rounded corners of the foundation were up to 1.5 inches thick and were likely to delaminate if a low shrinkage resin was not used. An E-glass fabric (type 7781) was employed with an epoxy resin system. A quasi-isotropic ply stacking sequence was employed with predominately 0 degree and 0/90 degree layers near the mid thickness with increasing +/-45 degree layers near the surfaces. The added thickness in the corners was obtained by tapering in 15 plys of 0/90 degree cloth. The tapered areas on the foundation were created by dropping plys from the center most regions.

The basic SCRIMP fabrication process was described earlier. For the foundation, however, a plug having the geometry of the foundation model was fabricated from plywood and high density plastic foam. A glass-epoxy mold was then cast over the plug to form a female mold. Peel ply and fabric were laid into the mold, a vacuum was pulled on the fabric stack, and resin was injected into the layup by means of the SCRIMP process. The part was then cured at 225 degrees F for two hours. At this point the part was demolded and trimmed, and a post cure to 300 degrees F was performed. A photograph of the completed foundation is shown in figure 15.

The fabrication costs for the foundation model are much higher than would be incurred in an actual production situation on a dollars per pound basis. Since it was the first structural application of this resin system in the SCRIMP process, some development work was required. In addition, the full cost of the plug and mold were included in the foundation cost instead of being amortized over several parts as would be the case in production. The small size of the model actually increased the difficulty of the layup process, especially in placing the fabric in the corner areas. The layup time could have also been reduced by substantially decreasing the number of layers. In fact, it is felt that a high quality full-scale structure could be fabricated using one-half the number of plies that were employed for the foundation model. The cost of the foundation model was approximately $90 per pound. It is estimated that full- scale foundations could be fabricated on a production basis for $20 to $40 per pound.

The strength of the composite foundation was evaluated by subjecting

it to high-impact shock tests (per MIL-S-901D) using a medium weight shock test machine. The foundation was tested in four different orientations: vertically, longitudinally, athwartships, and at an inclined angle of 30 degrees. The foundation, with a dummy steel mass to simulate the weight and center of gravity of supported equipment, is shown mounted in a vertical position on the medium weight shock machine in figure 16. Eight strain gages and from 2 to 5 accelerometers were recorded dynamically during each test. The foundation was tested both with and without resilient mounts which would be used between the foundation and the equipment bedplate on a full scale application. The composite foundation was able to sustain 16 impact blows, resulting in accelerations of up to 150 g's with no apparent degradation. In fact, eight additional tests were performed, going up to the maximum capacity of the test machine, to gain additional information on the integrity of the foundation. While a thorough examination has not yet been performed, there are no indications of structural degradation.

REPAIR USING 'SCRIMP'PROCESS

The above prototypes have clearly demonstrated the viability of the 'SCRIMP'process for the low-cost high-quality fabrication of these structures. It has also been recognized that it is important to demonstrate the effectiveness of the "SCRIMP' process when used as a repair procedure.

Such a capability has recently been successfully demonstrated on a sonar dome for the Hamilton Class of U.S. Coast Guard Cutters. These large GRP domes had been experiencing some delamination along the aft keel line upon internal pressurization with seawater. The Carderock Division, Naval Surface Warfare Center (CARDEROCKDIV) has been supporting the U.S. Coast Guard in investigating the cause of this delamination and in developing an improved structural dome configuration and repair procedure to correct the delamination problem. A structural modification to the dome has been developed which included increasing the radius of curvature at the bottom of the dome, increasing the laminate thickness from 0.75 inches to 1.0 inches, introducing + 45/-45 degree fabric plies into the 0/90 layup schedule, using vinyl ester resin instead of polyester to improve the toughness of the dome, and applying the 'SCRIMP' process. The repair procedure used on the dome is indicated in figure 17. The delaminated area was cutout, the laminate around the cutout was stepped back using a drop-off ratio of 20 to 1, and the stepped area was ground smooth. A male mold was then inserted into the cutout to provide a smooth contour for layup purposes. Dry glass fabric (9.6 oz.) was then 'scrimped' onto the dome in four steps, involving 28 plies per step. Four stages were required to minimize the development of wrinkles in the fabric under vacuum, and to allow them to be readily worked out when they did appear. After each step the applied laminate was allowed to cure at room temperature for 48 hours. After all 4 steps were complete, the repaired dome was allowed to post cure at 140 degrees F for 8 hours.

The repaired dome was subject to an internal pressurization to demonstrate that the repaired dome could withstand the required pressure of 17 psi without delamination. The dome actually withstood a pressure of 25 psi, approximately 50% higher than the design value

without any delamination.

The very successful repair demonstrated the capability for performing a high quality repair on a glass - polyester structure using a vinyl ester system. Although further tests are needed to validate the repair procedure for wider application, the results to date are very promising. The successful test also demonstrated that a thick laminate may be fabricated in stages using the 'SCRIMP' process. This has excellent implications for the multi- staged fabrication of thick (> 1 inch) composite structures for naval ship applications such as hulls.

POTENTIAL FUTURE APPLICATIONS

The excellent results to date with the 'SCRIMP' process for the deckhouse, mast, foundation and sonar dome structures, have stimulated interest in evaluating the process for application to the hulls of naval craft such as landing craft and patrol boats. Success could lead to the fabrication of hulls for smaller naval combatants, should they materialize in the future.

In an effort to evaluate the feasibility of using the 'SCRIMP' process for GRP hulls, CARDEROCKDIV intends to have a 0.35 scale validation model for a new landing craft concept, the Advanced Materiel Transporter (AMT), fabricated using this process. Under development for the U.S. Navy and Marine Corps, the full-scale AMT will be 126 feet long and 29 feet wide with a displacement of 249 long tons. The AMT will be capable of ballasting down and up to perform instream recovery of floating cargo and vehicles.

A hybrid structural design concept for the Validation Model and full scale AMT has been developed involving GRP single skin stiffened structure in the hull and balsa core sandwich structure in the deck and wing walls as shown in figure 18. The Validation Model will be constructed by fabricating the major structural elements, the hull, deck, transverse bulkheads and wing walls, using the 'SCRIMP' process and then assembling these elements using bolted and bonded joints. An effort will be made to lay up and scrimp the entire hull in a single step. If unsuccessful, the multi-step SCRIMP procedure used in the repair of the sonar dome will be applied. With the sonar dome procedure, dry GRP fabric will be laid down for one-half of the hull (transversely) and will be scrimped in place. After curing at room temperature for approximately 12 hours, the mold will be rotated and the process repeated. In this way, laminates of virtually any thickness may be built up. The GRP material will be overlapped along the keel for each stage of fabrication and should result in a primary - like bond based on the excellent results obtained in the sonar dome repair and test. In principle, it should be possible to use the 'SCRIMP' process to fabricate the 126 foot hull of the full scale AMT as a steppingstone to the hulls of larger naval craft in the future.

Some potentially near term applications for surface ships include composite maintenance enclosures, masts, and helicopter hangars. Near term submarine applications include the sail, control surfaces, sonar windows and stern cone. An agreement has recently been completed to fabricate a full scale model of a free flooding stern cone. This piece would be about 6 feet long and up to 1 inch thick and would be

fabricated in one piece (no joints). The proposed fabrication approach involves the placement of the fabric on a male mold, the insertion of the whole assembly into a female mold, the removal of the male mold, drawing the fiber pack against the female mold with a vacuum, and vacuum injection of the resin.

SUMMARY AND CONCLUSIONS

Over the last 3 years, the U.S. Navy has been successful in evaluating and demonstrating a low cost vacuum RTM process, referred to as SCRIMP, for the fabrication of high performance composite ship structures of aerospace quality.

Some of the advantages of the SCRIMP process include:

- Low cost due to the elimination of pre-pregging, manual wet out, expensive tooling and autoclaves.
- High quality and superior mechanical properties due to high glass content (70%) and extremely low void content (< 1%).
- Mechanical properties that are competitive with properties achieved using wet lay-up or prepreg with autoclave cure.
- Versatility for fabricating large composite monocoque, single skin stiffened, and sandwich structures using a variety of fibers and resins. Vinyl ester, polyester, epoxy and phenolic have been demonstrated.
- Projected low costs in production of $5 -$8/lb for GRP deckhouse structure, $20 to $30/lb for composite masts of hybrid glass/ carbon construction and $20 to $40/lb for composite foundations using a system of E- glass and epoxy resin.

Using the SCRIMP process, the capability has been demonstrated for the design and fabrication of composite ship structures including deckhouses, masts and foundations. A comparison of estimated weight and production costs for these composite applications versus conventional metallic structures are summarized in Table 5. It is seen that the composite deckhouse and foundation structures should be able to be fabricated at less cost than the corresponding metallic structures. Some of the capabilities for design and fabrication are highlighted below:

- Fabrication of large tapered (8'x16') hat-stiffened and sandwich deckhouse panels of aerospace quality in one step.
- Fabrication of thick, geometrically complex, monocoque structure for masts and foundations.
- Design of affordable composite ship structures that meet air blast and shock requirements.
- Development of hybrid GRP/ steel structure to maximize structural performance and shipyard producibility.
- Repair of thick monocoque GRP structures.
- Multi- stage scrimping of thick laminates for potential application to the construction of large GRP hulls.

ACKNOWLEDGMENTS

The authors are grateful to Mr. S. Bartlett and Mr. P. Potter of CARDEROCKDIV and Mr. W. Seemann of Seemann Composites for their technical contributions to this paper. Appreciation is also expressed to Dr. J. Corrado of CARDEROCKDIV, Mr. J. Gagorik and Mr. J. Remmers of the Office of Naval Technology, Mr. A. Kurzweil of the Naval Sea Systems Command, Dr. T. Tsai of the Defense Nuclear Agency, and Mr. T. Powell of the U.S. Coast Guard for their endorsement and support of these research and development programs.

REFERENCES

1. Greene, E. " Use of Fiberglass Reinforced Plastics in the Marine Industry", Ship Structure Committee Report, SSC 360, June 1990.

2. " Resin Transfer Molding for Advanced Composites ", Advanced Composites, pg. 60, March/ April 1990.

3. Strong, A. Brent, Fundamentals of Composite Manufacturing: Materials, Methods and Applications, Society of Manufacturing Engineers, 1989.

4. " Injection Moulding for Large Craft", Ship and Boat International, January/ February 1986.

5. Critchfield, M.O., S.L. Morgan, P.C. Potter, " GRP Deckhouse Development for Naval Ships ", Advances in Marine Structures - 2, Elsevier Applied Science, pg. 372, 1991.

6. Smith,C.S. and P. Murphy, " Response of Hybrid GRP/ Steel Superstructures to Blast Loading - Theory and Experiment", Advances in Marine Structures - 2, Elsevier Applied Science, pg. 392, 1991.

Table 1 - Known Vacuum RTM Processes

COMPANY	PROCESS	APPLICATION
• SEEMANN COMPOSITES, INC.	SCRIMP	DECKHOUSE, MAST, FOUNDATION SONAR DOME, RIB HULL STRUCTURE
• DOUGLAS AIRCRAFT CORP.	VACUUM IMPREGNATION	THREE STRINGER WING PANELS
• JEREMY ROGERS, UK	VARI	36' RACING BOATS (4) 34' PRODUCTION BOATS (≈15) 40'+PRODUCTION BOATS (≈25)
• LE COMPTE HOLLAND BV	VACUUM ASSISTED INJECTION MOLDING	22M LANDING CRAFT
• AMI, INC.	PRESTO-VAC	TRUCK AIR SHIELDS

Table 2 - Mechanical Property Comparison (Hand Lay-up vs. SCRIMP vs. Autoclave)

PROPERTY	HAND LAY-UP[1] 50%* POLY WR	SCRIMP[1] 70%* POLY WR	SCRIMP[1] 70%* VINYL WR	SCRIMP[2] 70%* VINYL CLOTH	PRE-PREG[2] AUTOCLAVE EPOXY CLOTH	SCRIMP[3] 70%* VINYL 3-TO-1	WET LAY-UP AUTOCLAVE POLY 3-TO-1
TENSILE STRENGTH (ksi)	46.8	67.3	70.9	–	–	109.7	111.1
TENSILE MODULUS (msi)	3.2	4.5	4.6	–	–	5.5	5.5
COMPRESSIVE STRENGTH (ksi)	39.1	42.1	68.6	61.0	60.0	67.6	78.2
FLEXURAL STRENGTH (ksi)	52.2	66.8	90.0	82.0	75.0	121.4	–
INTERLAMINAR SHEAR STRENGTH (ksi)	3.3	4.5	7.3	7.2	8.5	6.8	3.3

[1] 24 oz WOVEN ROVING
[2] 8 HARNESS SATIN CLOTH
[3] TWILL WEAVE

* APPROXIMATE BY WEIGHT

Table 3 - Comparison of Structural Performance for Deckhouse Modules

MODULE	MAX./ALLOWABLE DEFLECTION	MAX./ALLOWABLE STRAIN
GRP STIFFENED	0.51 (*) 1.12 (**)	0.50 (*) 0.87 (**)
GRP SANDWICH	0.96 (***)	0.96 (***)

(*) MISERS GOLD EVENT (DESIGN PRESSURE)
(**) DISTANT IMAGE EVENT (2 x DESIGN PRESSURE)
(***) DISTANT IMAGE EVENT (DESIGN PRESSURE)

ALLOWABLE STRAIN = ULTIMATE STRAIN/1.25
ALLOWABLE DEFLECTION = 5.0 INCHES

Table 4 - Weight and Cost Comparison for Deckhouse Modules

DECKHOUSE MODULE	PANEL AREAL WEIGHT (lb/ft^2)	MODULE WEIGHT (lb)	PANEL COST		MODULE COST ($K)
			($/lb)	($/$ft^2$)	
HAT STIFFENED	8.4	6500	9.40	78.60	87.5
FIRE-HARDENED SANDWICH	6.5	5400	15.90	103.50	89.1

Table 5 - Weight and Cost Comparison for Metallic vs. Composite Ship Structures

ITEM	COMPARISON	WT SAVINGS FOR COMPOSITES	FABRICATION COST [$/LB]*		COMPONENT COST [$COMPOSITE/$METAL]**
			STEEL OR ALUMINUM	COMPOSITES	
DECKHOUSES	STEEL	35-45%	4-6	5-8	0.8
MASTS	ALUMINUM	20-50%	9-12	20-30	1.5
FOUNDATIONS	STEEL	UP TO 60%	10-40	20-40	0.5

* ASSUMES COMPOSITES IN FULL PRODUCTION
** BASED ON AVERAGE WEIGHT AND COST SAVINGS

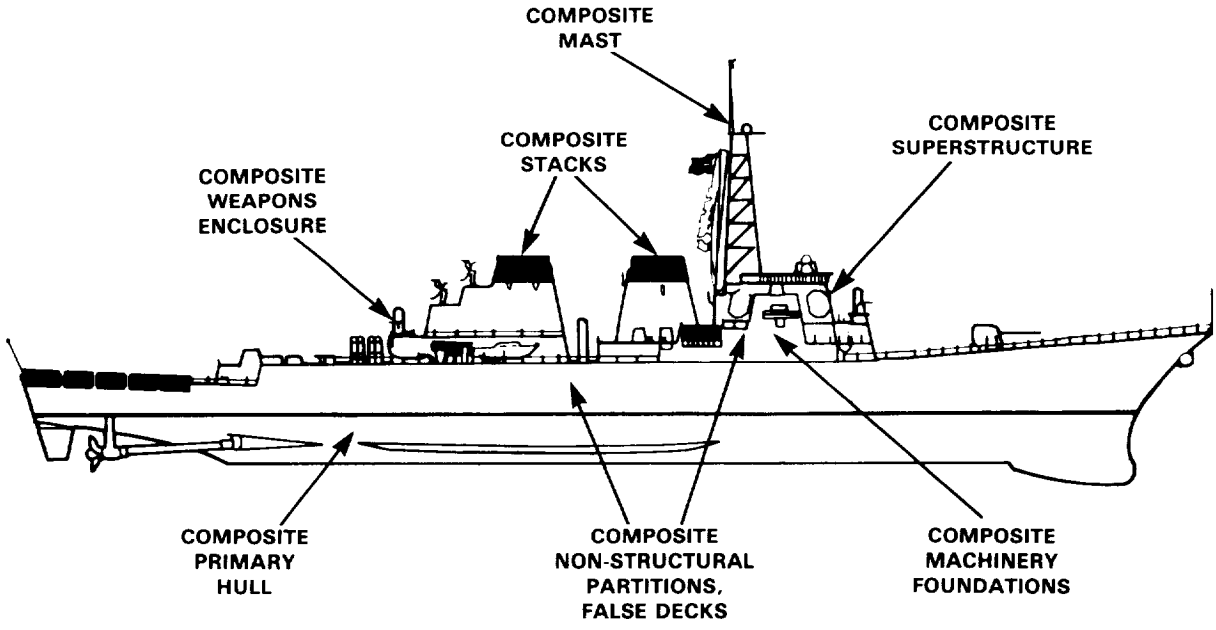

Figure 1 - Potential Surface Ship Applications of Composite Structures

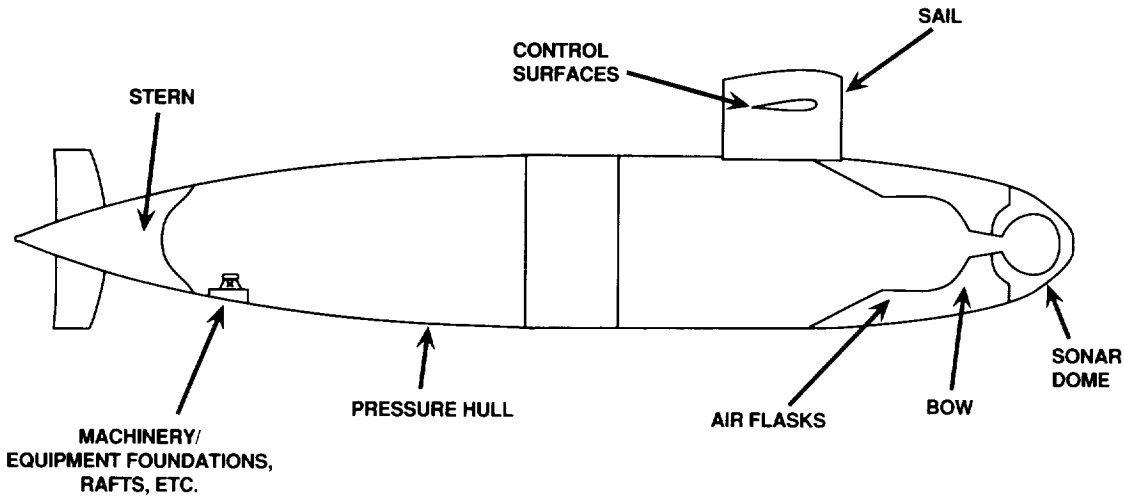

Figure 2 - Potential Submarine Applications of Composite Structures

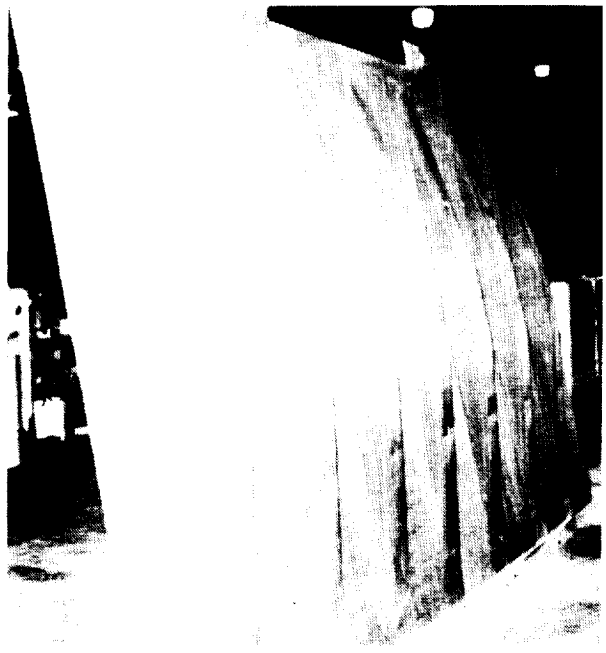

Figure 3. Photograph of GRP Stiffened Deckhouse Panel

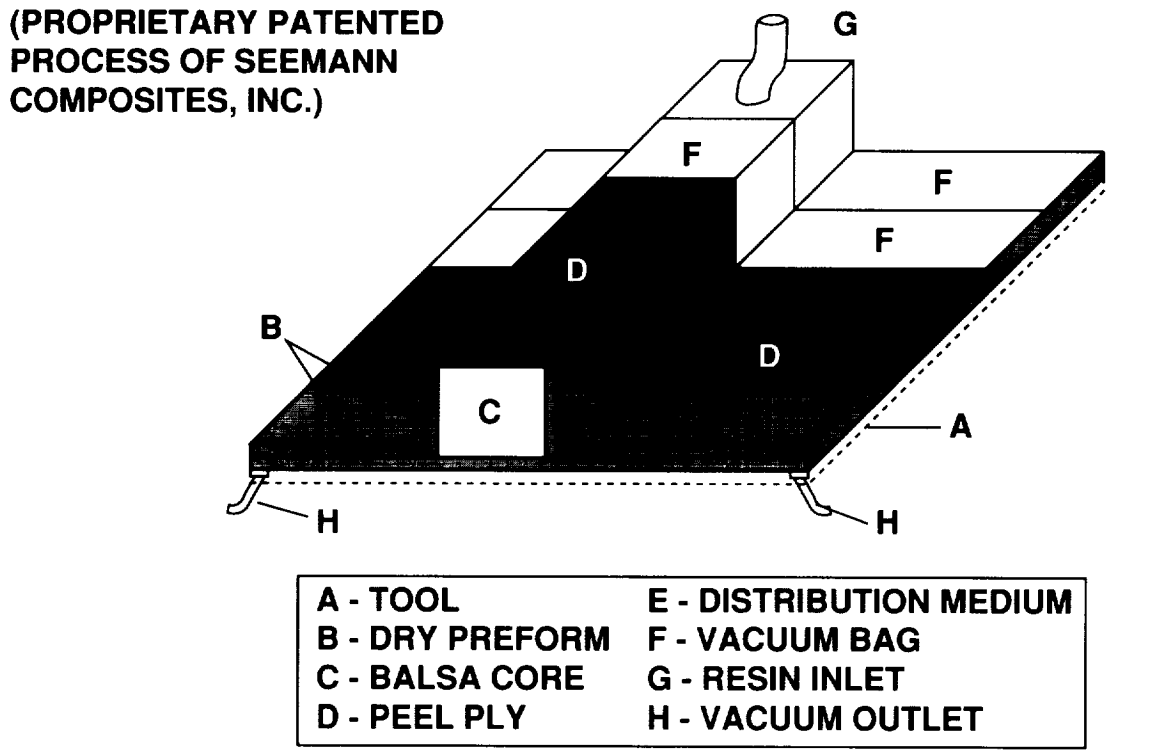

Figure 4 - SCRIMP Process for Single Skin Stiffened Panel

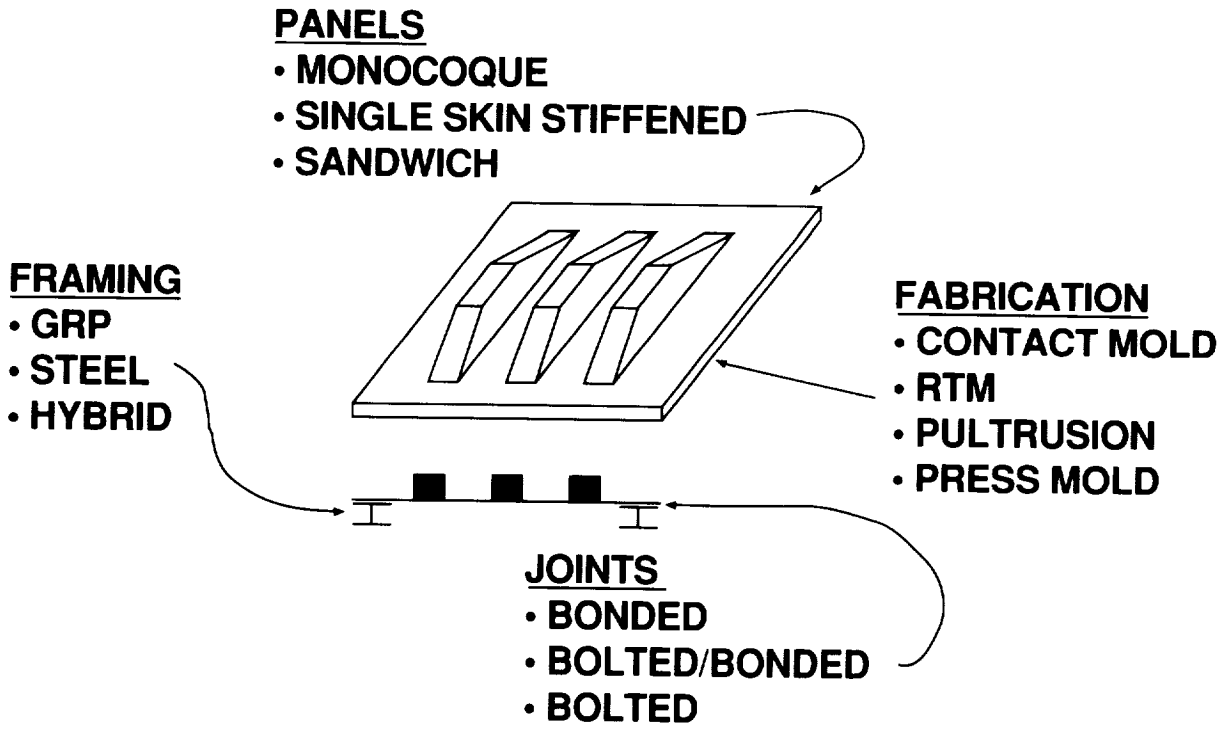

Figure 5 - Design/Fabrication Options for Composite Deckhouse Panels

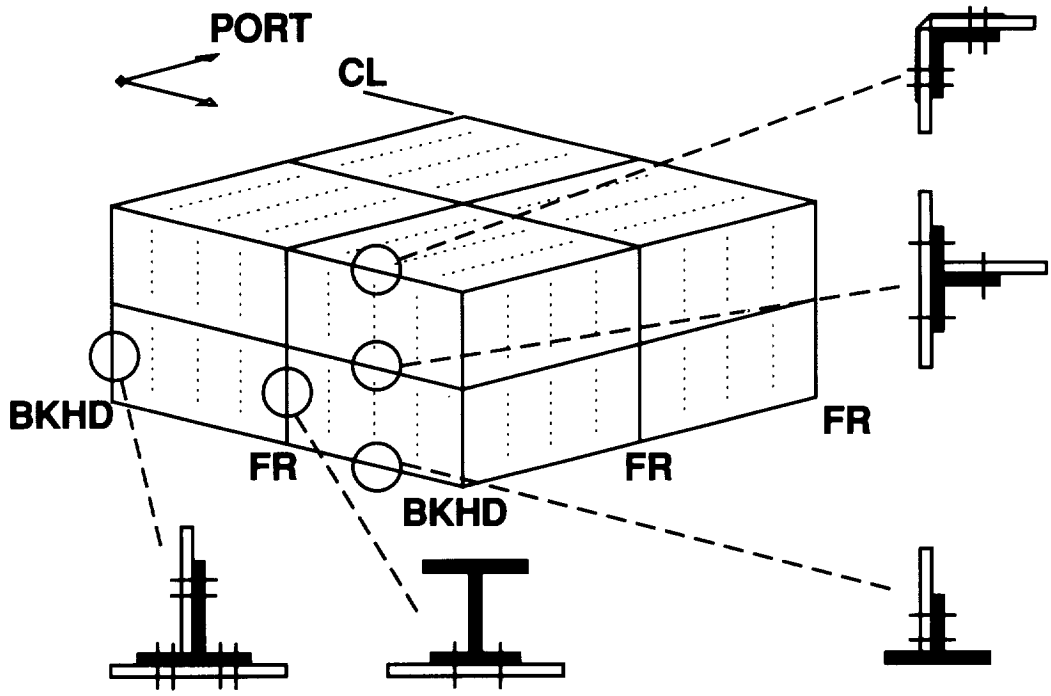

Figure 6 - Joint Details for GRP Deckhouse

(a) Exterior View of Deckhouse Module

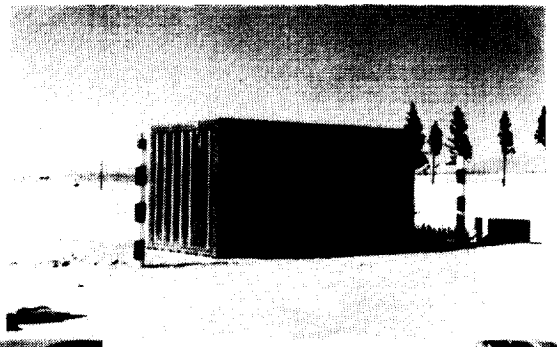

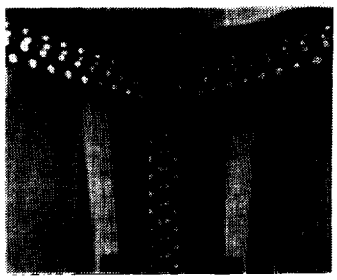

(b) Inside Corner of Stiffened Module

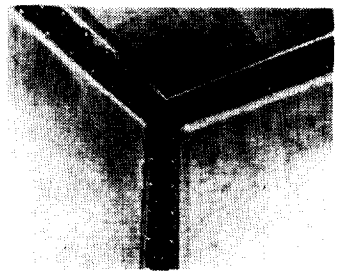

(c) Inside Corner of Sandwich Modules

Figure 7. Photographs of GRP Stiffened and Sandwich Modules

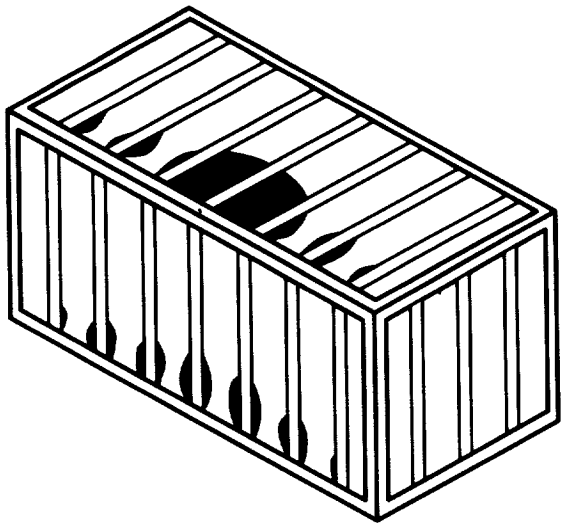

Figure 8. Delamination Map For GRP Stiffened Module

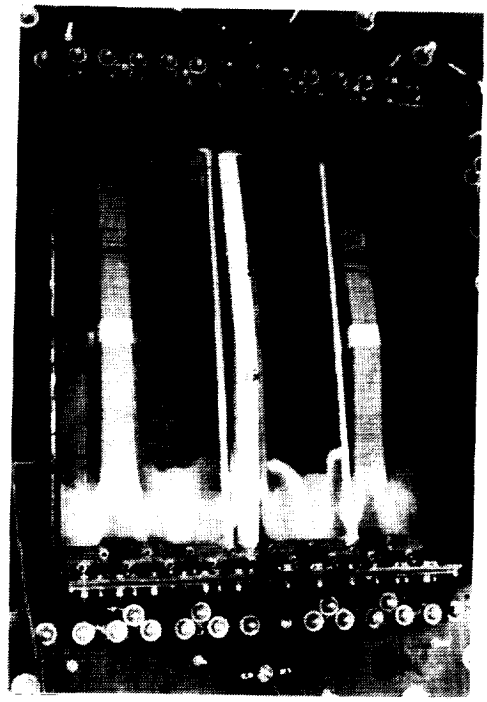

Figure 9. One-Half Scale Deckhouse Panel After Blast Tube Test

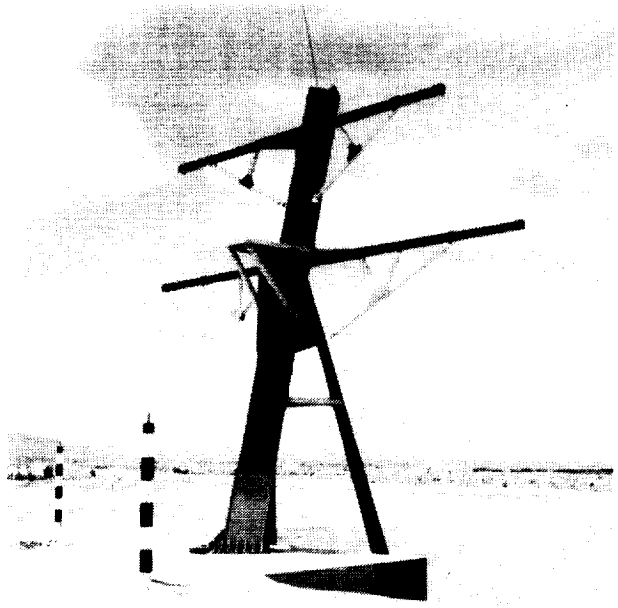

Figure 10. Photograph of One-Half Scale Composite Mast

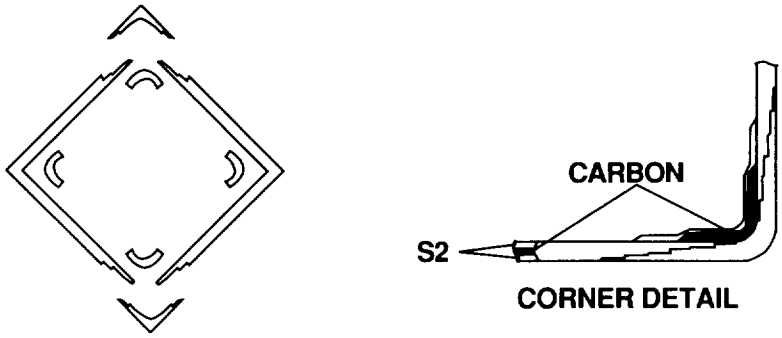

Figure 11 - Materials and Fabrication Details for Main Trunk

Figure 12 - Typical Cross-Section for Aft Legs and Yard Arms

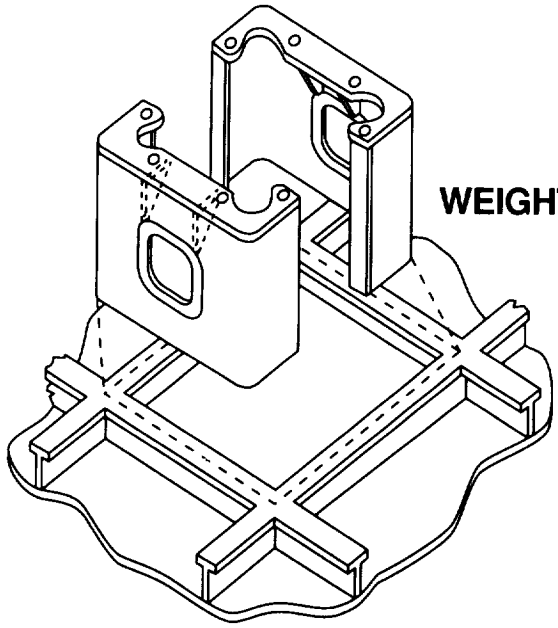

Figure 13 - Steel Fresh Water Pump Foundation

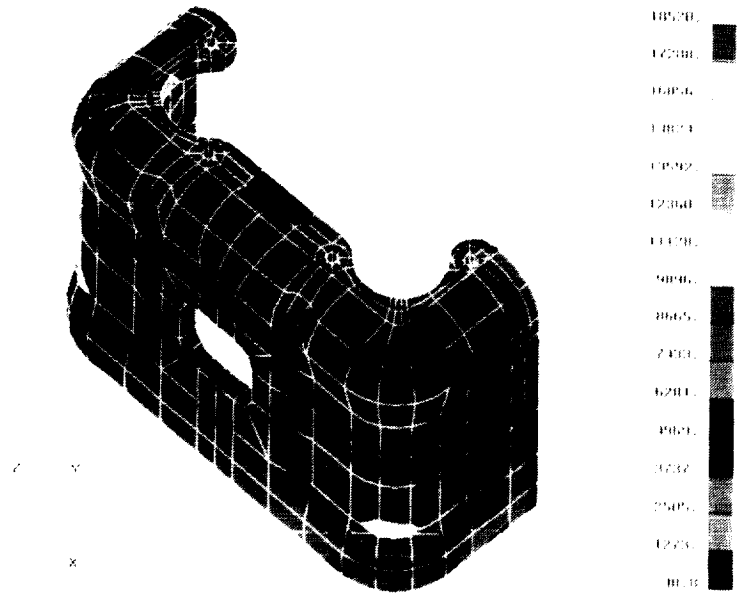

Figure 14. Stress Distribution in Composite Foundation

Figure 15. Photograph of Composite Submarine Pump Foundation (1/2 Scale)

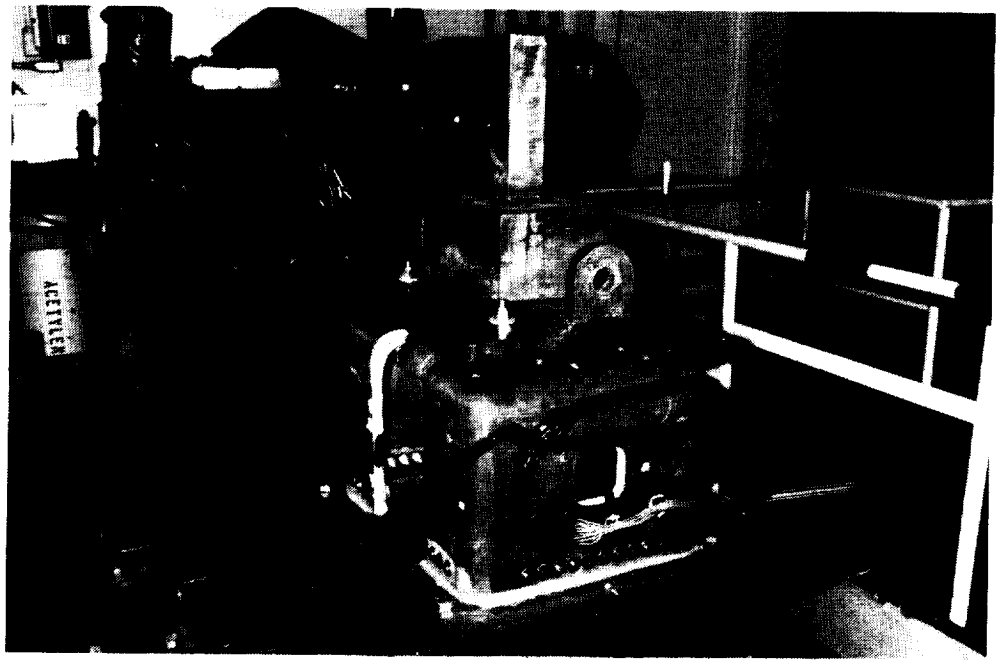

Figure 16. Composite Foundation on Medium Weight Shock Machine

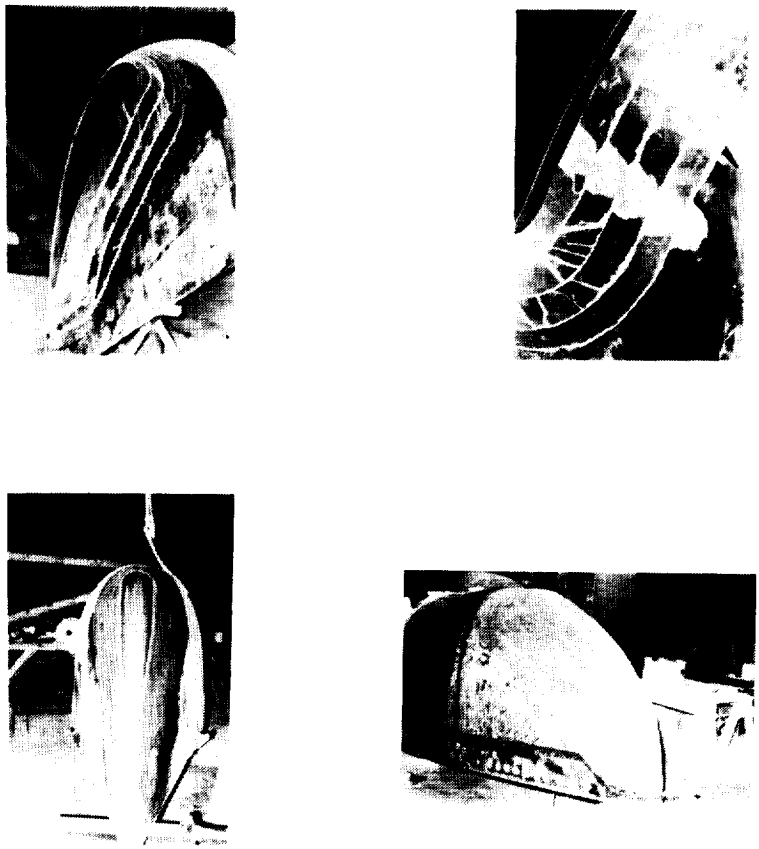

Figure 17. Repair of GRP Sonar Dome

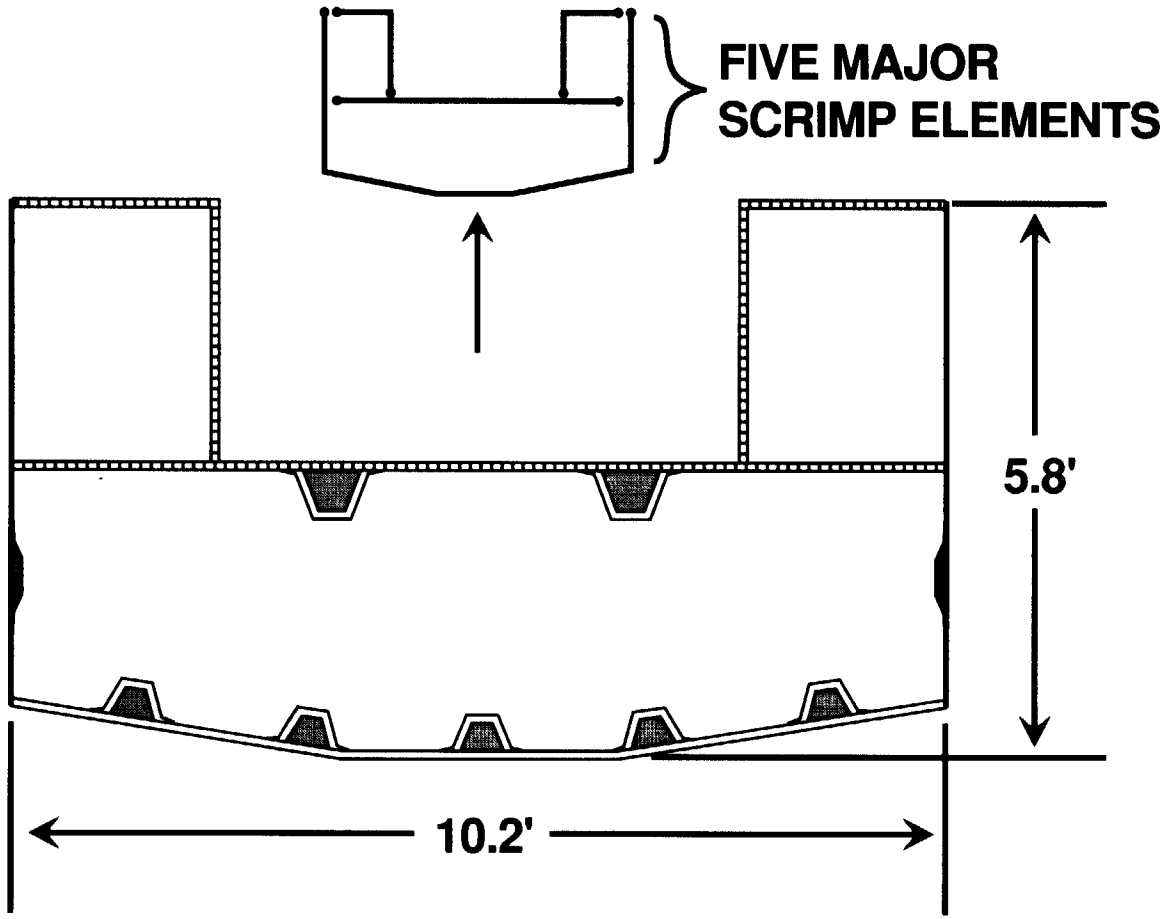

Figure 18 - Midship Design for Advanced Materiel Transporter

SESSION X

AIRCRAFT DESIGN METHODOLOGY (B)

THIS PAGE INTENTIONALLY BLANK